CO Oxidation on Pd(100) and Pd(111): A Comparative Study of Reaction Pathways and Reactivity at Low and Medium Coverages

C. J. Zhang and P. Hu*

Contribution from the School of Chemistry, The Queen's University of Belfast, Belfast BT9 5AG, United Kingdom

Received July 5, 2000. Revised Manuscript Received October 10, 2000

Abstract: We have performed density functional theory calculations with the generalized gradient approximation to investigate CO oxidation on a close-packed transition metal surface, Pd(111), and a more open surface, Pd(100), aiming to shed light on surface structure effects on reaction pathways and reactivity, an important issue in catalysis. Reaction pathways on both surfaces at two different coverages have been studied. It is found that the reaction pathways on both surfaces possess crucial common features despite the fact that they have different surface symmetries. Having determined reaction barriers in these systems, we find that the reaction on Pd(111) is strongly coverage dependent. Surface coverages, however, have little effect on the reaction on Pd(100). Calculations also reveal that the low coverage reactions are structure sensitive while the medium coverage reactions are not. Detailed discussions on these results are given.

1. Introduction

Catalytic CO oxidation has been a hot topic in the last three decades due to its important applications in many technologies such as car-exhaust emission control and CO_2 lasers.[1−14] Because of its relative simplicity, being widely considered as a model system to study heterogeneous catalysis, CO oxidation has recently drawn much attention theoretically. The theoretical studies mainly by means of density functional theory (DFT)[15−23] have focused on the identification of transition states (TSs) and reaction pathways, with the aim of providing microscopic insights into the reaction processes. Very recently, Zhang, Hu, and Alavi[21] have proposed a general reaction mechanism for CO oxidation on close-packed transition metal surfaces based on the results of DFT calculations. Two crucial events in the reaction pathways have been suggested:[21] (i) the adsorbed O atom must be activated from the initial hollow chemisorption site and (ii) the CO molecule has to approach the O atom in the correct direction. These studies, however, have focused on the close-packed metal surfaces and to date no study on a more open surface has appeared. The following interesting questions remain to be answered: What are the reaction channels for CO oxidation on more open surfaces? Are there any differences in reaction pathways between the close-packed and more open surfaces? In addition, the structure−reactivity relationship has long been an important issue in heterogeneous catalysis.[24−30] Despite the large volume of work devoted to the understanding of this relationship, the physical origin of the role of structure effects on reactivity remains unclear.

We report in this paper a DFT study on the reaction mechanisms for CO oxidation on Pd(111) and a more open surface, Pd(100), at different adsorbate coverages, aiming to obtain a clear understanding of two important issues in heterogeneous catalysis: (i) surface structure effects on reaction pathways and (ii) surface structure effects on reactivity. Although this study has focused on the catalytic CO oxidation mechanism on Pd surfaces, it is concerned with the basic events involved in surface processes and is therefore of general chemical interest.

The adsorption of CO and O on palladium surfaces has been extensively studied[31−41] and the adsorption structures for both

* Address correspondence to this author. Fax: (+44) 28 90382117. E-mail: p.hu@qub.ac.uk.

(1) Engel, T.; Ertl, G. *Adv. Catal.* **1979**, *28*, 1.
(2) Engel, T.; Ertl, G. In *The Chemical Physics of Solid Surfaces and Heterogeneous Catalysis*; King, D. A., Woodruff, D. P., Eds.; Elsevier: New York, 1982; Vol. 4.
(3) Campbell, C. T.; Ertl, G.; Kuipers, H.; Segner, J. *J. Chem. Phys.* **1980**, *73*, 5862.
(4) Gland, J. L.; Kollin, E. B. *J. Chem. Phys.* **1983**, *78*, 983.
(5) Matsushima, T. *Surf. Sci.* **1983**, *127*, 403.
(6) Kwong, D. W. J.; Leon, N. de; Haller, G. L. *Chem. Phys. Lett.* **1988**, *144*, 533.
(7) Kaukonen, H.-P.; Nieminen, R. M. *J. Chem. Phys.* **1989**, *91*, 4380.
(8) Mieher, W. D.; Ho, W. *J. Chem. Phys.* **1993**, *99*, 9279.
(9) Ertl, G. *Surf. Sci.* **1994**, *299*, 742.
(10) Allers, K. H.; Pfnür, H.; Feulner, P.; Menzel, D. *J. Chem. Phys.* **1994**, *100*, 3985.
(11) Tripa, C. E.; Arumaninayagam, Ch. R.; Yates, J. T. *J. Chem. Phys.* **1996**, *105*, 1691.
(12) Yeo, Y. Y.; Vattuone, L.; King, D. A. *J. Chem. Phys.* **1997**, *106*, 392.
(13) Wintterlin, J.; Völkening, S.; Janssens, J. V. W.; Zambelli, T.; Ertl, G. *Science* **1997**, *278*, 1931.
(14) Valden, M.; Lai X.; Goodman, D. W. *Science* **1998**, *281*, 1647.
(15) Stampfl, C.; Scheffler, M. *Phys. Rev. Lett.* **1997**, *78*, 1500.
(16) Alavi, A.; Hu, P.; Deutsch, T.; Silvestrelli, P. L.; Hutter, J. *Phys. Rev. Lett.* **1998**, *80*, 3650.
(17) Stampfl, C.; Scheffler, M. *J. Vac. Sci. Technol. A* **1997**, *15*, 1635.
(18) Stampfl, C.; Scheffler, M. *Surf. Sci.* **1997**, *377*, 808.
(19) Eicher, A.; Hafner, J. *Phys. Rev. B* **1999**, *59*, 5960.
(20) Eicher, A.; Hafner, J. *Surf. Sci.* **1999**, *435*, 58.
(21) Zhang, C. J.; Hu, P.; Alavi, A. *J. Am. Chem. Soc.* **1999**, *121*, 7931.
(22) Zhang, C. J.; Hu, P.; Alavi, A. *J. Chem. Phys.* **2000**, *112*, 10564.
(23) Zhang, C. J.; Hu, P. *J. Am. Chem. Soc.* **2000**, *122*, 2134.
(24) Goodman, D. W. *J. Phys. Chem.* **1996**, *100*, 13090.
(25) Vesecky, S. M.; Chen, P.; Xu, X.; Goodman, D. W. *J. Vac. Sci. Technol. A* **1995**, *13*, 1539.
(26) Vesecky, S. M.; Rainer, D. R.; Goodman, D. W. *J. Vac. Sci. Technol. A* **1996**, *14*, 1457.
(27) Goodman, D. W.; Peden, C. H. F. *J. Phys. Chem.* **1986**, *90*, 4839.
(28) Peden, C. H. F.; Goodman, D. W. *J. Phys. Chem.* **1986**, *90*, 1360.
(29) Sajkowski, D. J.; Boudart, M. *Catal. Rev.* **1987**, *29*, 325.
(30) Boudart, M.; Rumpf, F. *React. Kinet. Catal.* **1987**, *L 35*, 95.
(31) Conrad, H.; Ertl, G.; Küppers, J. *Surf. Sci.* **1978**, *76*, 323.
(32) Matsushima, T.; Asada, H. *J. Chem. Phys.* **1986**, *85*, 1658.

10.1021/ja002432f CCC: $20.00
Published on Web 01/19/2001

O and CO have been well established. It was found experimentally by using a variety of surface analysis techniques[33−35] that CO molecules adsorb on bridge sites on Pd(100). Studies on O adsorption on Pd(100)[36,37] suggested that the O atom prefers the 4-fold hollow site. On the Pd(111) surface, it was found that both CO and O preferentially adsorb at 3-fold hollow sites.[38−41] In addition, quite a few experimental studies have been devoted to the investigation of the kinetics of CO oxidation on Pd.[42−46] For example, Szanyi and Goodman[46] studied CO oxidation on Pd(100) using an elevated-pressure IR cell/ultrahigh vacuum surface analysis system. They estimated an activation energy of 29.4 ± 0.3 kcal/mol (123 kJ/mol, 1.2 eV) for the reaction taking place between 500 and 575 K at a total pressure of 1.50 Torr of CO and O_2. By using the molecular beam technique, Engel and Ertl[42] investigated CO oxidation on Pd(111) and suggested a range of activation energies (25 kcal/mol (105 kJ/mol, 1.08 eV) to 14 kcal/mol (59 kJ/mol, 0.61 eV) for CO coverage between ≤0.02 monolayer (ML) and 0.33 ML on an O-precovered surface). However, the microscopic reaction processes on these surfaces remain unknown. In this study we have identified transition states for CO oxidation on both Pd(111) and Pd(100) surfaces at low and medium coverages. A detailed comparison of the reaction pathways and the reactivity between these two different surfaces has been made to shed some light on the structure−reactivity issue.

The paper is organized as follows: In section 2, some details of our calculations are outlined. Following this, reaction pathways for CO oxidation on Pd(111) in both p(2 × 2) and p(3 × 2) unit cells are presented. In sections 3.3 and 3.4, results on Pd(100) also in p(2 × 2) and p(3 × 2) unit cells are shown. A comparison between the reaction pathways obtained on these two surfaces is made in the first part of the discussion section and the structure−reactivity relationship is considered in the second part of the discussion section. Finally, our conclusions are summarized in the last section.

2. Calculations

DFT calculations within the generalized gradient approximation[47] were carried out to study reaction mechanisms for CO oxidation on Pd(100) and Pd(111). The total energy program, CASTEP,[48] was used throughout to obtain optimized structures and energies. Ionic cores were described by ultrasoft pseudopotentials[49] and the Kohn−Sham one-electron states were expanded in a plane wave basis set up to 300 eV. A Fermi smearing of 0.1 eV was utilized, and the corrected energy was extrapolated to zero temperature by the method of Gillan and De Vita,[50,51] which considerably reduces the **k**-point sampling. The supercell approach was employed to model periodic geometries. The surfaces were modeled by four- and three-layer slabs of Pd atoms for (100) and (111) surfaces, respectively. In all the calculations, the bottom three and two layers of Pd atoms for (100) and (111) surfaces, respectively, were held fixed in their bulk positions, while the top layer of metal atoms was allowed to relax. As shown in recent work,[21−23,52−56] the above setup provides sufficient accuracy. For Pd(100) and Pd(111), both p(2 × 2) and p(3 × 2) unit cells have been considered. 2 × 2 × 1 and 2 × 3 × 1 **k**-grid samplings within the surface Brillouin zones were used in p(2 × 2) and p(3 × 2) unit cells, respectively. We have tested the **k**-point sampling by using 4 × 4 × 1 and 3 × 4 × 1 Monkhorst−Pack meshes[57] for these two unit cells and found the error of the calculated energies to be less than 0.1 eV.

TSs were searched using a constrained optimization scheme.[16,21−23] In this approach, the distance between C of CO and the adsorbed O (O_a) was fixed and the rest of the degrees of freedom were optimized according to the forces calculated from the Hellmann−Feynman theorem. This procedure was repeated at different C−O_a distances until the following conditions were reached: (i) all forces on atoms vanish and (ii) the total energy is a maximum with respect to the reaction coordinate (the C−O_a distance) and a minimum with respect to all other degrees of freedom.

3. Results

3.1. CO Oxidation on Pd(111) at an O Coverage of 1/4 ML. It was reported experimentally[31] that depending on the exposure of gases, two different phases of CO and O_a coadsorption could form on Pd(111). One is separate ($\sqrt{3}\times\sqrt{3}$)-*R*30°−CO and ($\sqrt{3}\times\sqrt{3}$)*R*30°−O_a domains and another is the mixed (2 × 1)−(CO + O_a) phase. The mixed (2 × 1)−(CO + O_a) phase was recently shown to exist as separate (2 × 1)−CO and (2 × 1)−O_a domains.[58] To model CO oxidation on Pd(111) at medium local coverages between the (2 × 1)−CO domain and the (2 × 1)−O_a domain, we carried out simulations for CO oxidation on Pd(111) with one CO molecule and one O_a atom in a p(2 × 2) unit cell. This model has the same surface coverages of CO and O_a as the (2 × 1)−CO and (2 × 1)−O_a domains. The validity of this model will be discussed at the end of this subsection. In this model, both the O_a and the CO coverages are 1/4 ML (this will hereafter be referred to as the 1/4 ML system). Structure optimizations for the initial states of the reaction were carried out. The most stable initial state was found to be one with both O_a and CO on fcc hollow sites (Figure 1). Calculated chemisorption energies of O_a and CO in this initial state together with the relevant data reported in the literature[59,60] are listed in Table 1. It is worth mentioning that a recent ion scattering study[41] revealed that O_a adsorbs preferentially on the hcp hollow site of Pd(111). However, we found the hcp site to be about 0.25 eV less stable than O_a chemisorption on the fcc hollow site. Our result is consistent with a recent DFT study.[59] Furthermore, Over and co-workers[58] performed very recently a LEED analysis and DFT calculations for O chemisorption on Pd(111) and found that the fcc site is favored for O chemisorption, which is again consistent with our result. Therefore, a reanalyzis of the ion scattering data is required.

Having determined the most stable initial state, several possible pathways for the reaction have been searched. Two

(33) Bradshaw, A. M.; Hoffmann, F. M. *Surf. Sci*. **1978**, *72*, 513.
(34) Tracy, J. C.; Palmberg, P. W. *J. Chem. Phys*. **1969**, *51*, 4852.
(35) Behm, R. J.; Christmann, K.; Ertl, G.; Van Hove, M. A. *J. Chem. Phys*. **1980**, *73*, 2984.
(36) Chang, S. -L.; Thiel, P. A. *Phys. Rev. Lett*. **1987**, *59*, 296.
(37) Chang, S.-L.; Thiel, P. A. *J. Chem. Phys*. **1988**, *88*, 2071.
(38) Hoffmann, F. M. *Surf. Sci. Rep*. **1983**, *3*, 107.
(39) Conrad, H.; Ertl, G.; Koch, J.; Latta, E. E. *Surf. Sci*. **1974**, *43*, 462.
(40) Imbihl, R.; Demuth, J. E. *Surf. Sci*. **1986**, *173*, 395.
(41) Steltenpohl, A.; Memmel, N. *Surf. Sci*. **1999**, *443*, 13.
(42) Engel, T.; Ertl, G. *J. Chem. Phys*. **1978**, *69*, 1267.
(43) Stuve, E. M.; Madix, R. J.; Brundle, C. R. *Surf. Sci*. **1984**, *146*, 155.
(44) Berlowitz, P. J.; Peden, C. H. F.; Goodman, D. W. *J. Phys. Chem*. **1988**, *92*, 5213.
(45) Ohno, Y.; Matsushima, T.; Shobatake, K. *Surf. Sci*. **1992**, *273*, 291.
(46) Szanyi, J.; Goodman, D. W. *J. Phys. Chem*. **1994**, *98*, 2972.
(47) Perdew, J. P. *Phys. Rev. B* **1986**, *33*, 8822. Becke, A. D. *Phys. Rev. A* **1988**, *38*, 3098.
(48) Payne, M. C.; Teter, M. P.; Allen, D. C.; Arias, T. A.; Joannopolous, J. D. *Rev. Mod. Phys*. **1992**, *64*, 1045.
(49) Vanderbilt, D. *Phys. Rev. B* **1990**, *41*, 7892.
(50) Gillan, M. J. *J. Phys. Condens. Matter* **1989**, *1*, 689.
(51) De Vita, A.; Gillan, M. J. *J. Phys. Condens. Matter* **1991**, *3*, 6225.
(52) Zhang, C. J.; Hu, P.; Lee, M.-H. *Surf. Sci*. **1999**, *432*, 305.
(53) Michaelides, A.; Hu, P.; Alavi, A. *J. Chem. Phys*. **1999**, *111*, 1343.
(54) Michaelides, A.; Hu, P. *J. Chem. Phys*. **2000**, *112*, 6006.
(55) Lynch, M.; Hu, P. *Surf. Sci*. **2000**, *458*, 1.
(56) Michaelides, A.; Hu, P. *Surf. Sci*. **1999**, *437*, 362.
(57) Monkhorst, H. J.; Pack, J. D. *Phys. Rev. B* **1976**, *13*, 5188.
(58) Seitsonen, A. P.; Kim, Y. D.; Schwegmann, S.; Over, H. S*urf. Sci.* **2000**, submitted for publication.
(59) Loffreda, D.; Simon, D.; Sautet, P. *J. Chem. Phys*. **1998**, *108*, 6447.
(60) Hammer, B.; Hansen, L. B.; Nørskov, L. K. *Phys. Rev. B* **1999**, *59*, 7413.

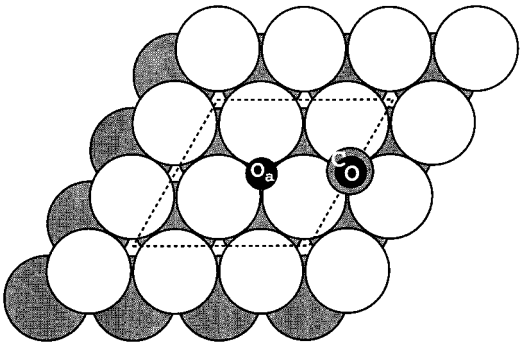

Figure 1. Top view of the most stable structure of Pd(111)−p(2 × 2)−(CO + O_a). The large white circles and the large gray circles represent the first and second layer of Pd atoms, respectively. The small gray circle and small dark circles indicate C and O atoms, respectively. The unit cell in the surface plane is indicated with dotted lines.

Table 1. Chemisorption Energies of O_a and CO in Pd(111)−p(2 × 2)−(CO + O_a) and Pd(111)−p(3 × 2)−(CO + O_a), Where O_a Is the Chemisorbed O Atom[a]

	chemisorption energy (eV)	
	O_a	CO
Pd(111)−p(2 × 2)−(CO + O_a)		
CO fcc hollow; O_a fcc hollow	3.66	1.60
Pd(111)−p(3 × 2)−(CO+O_a)		
1 CO top; O_a fcc hollow	4.20	1.43
2 CO another top; O_a fcc hollow	4.25	1.48
3 CO bridge; O_a fcc hollow	4.21	1.95
4 CO hcp hollow; O_a fcc hollow	4.18	2.13
Pd(111)−p($\sqrt{3} \times \sqrt{3}$)*R*30°−O(fcc)[b]	4.15	
Pd(111)−p(2 × 2)−O(fcc)[c]	4.08	
Pd(111)−p(2 × 2)−CO(fcc)[c]		2.07

[a] The CO chemisorption energies presented in each unit cell are for CO chemisorption upon an O_a precovered Pd(111) surface with the same unit cell. It can be calculated from the following: $\Delta E_{CO} = E_{CO/Oa/Pd} - E_{Oa/Pd} - E_{CO}$, where $E_{CO/Oa/Pd}$, $E_{Oa/Pd}$, and E_{CO} are the total energies of the coadsorption system, a pure O_a adsorption system, and a CO molecule, respectively. Likewise, the O_a Chemisorption energies are defined and calculated in a similar manner. In the p(3 × 2) unit cell, there are four possible coadsorption structures with low energies corresponding to those shown in Figure 3. For comparison, some relevant data from the literature are also listed. [b] Reference 59. [c] Reference 60.

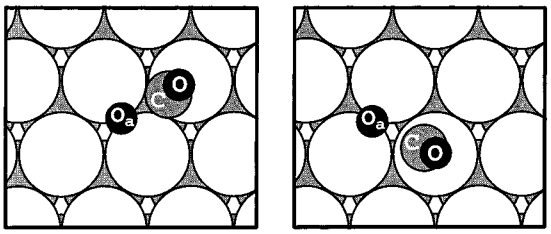

Figure 2. Two distinct transition state geometries for CO oxidation on Pd(111). The main structural parameters are listed in Table 2.

distinct TSs have been identified, as shown in Figure 2. The main structural parameters of these TSs are summarized in Table 2. It can be seen that these two TSs are very similar in nature to each other: The O_a atom is close to a bridge site and the CO is on an off-top site, tilting away from the O_a atom. In fact, they are also very similar to the TSs determined for CO oxidation on Pt(111), Ru(0001), and Rh(111).[16,21−23] Recently, we have determined low-energy reaction pathways for CO oxidation on these surfaces and a general mechanism on close-packed transition metal surfaces has been proposed.[21] A CO oxidation process can be divided into three distinguished periods.

Table 2. The Main Geometrical Parameters of the TSs Identified for CO Oxidation on Pd(111) in p(2 × 2) and p(3 × 2) Unit Cells and the Reaction Barriers Associated with These TSs

	barrier (eV)	C−O_a (Å)	C−Pd (Å)	C−O (Å)	∠O_a−C−O (Å)
TS(a)					
1/4 ML	0.93	1.80	1.96	1.17	114.4
1/6 ML	1.49	1.80	1.98	1.17	113.1
TS(b)					
1/4 ML	1.02	2.03	1.93	1.16	110.9

First, a CO molecule moves quite freely from its initial position, while an O_a vibrates around its 3-fold hollow position. The energy change in this period is very small. Second, the O_a becomes activated and moves toward a bridge site. If the CO moves toward the O_a in the correct direction, then a TS can be achieved. In this period, the energy increases dramatically. Third, the O_a and the CO move toward each other, forming a CO_2. At the same time, the O_a and the CO move away together from the TS toward a low coordination site. It was concluded that the key event for CO oxidation is the activation of O_a from the 3-fold hollow site. Indeed, it is expected that these features will also be true in the case of CO oxidation on Pd(111), given the similarity of the TSs shown in Figure 2 to the TSs identified on Pt(111), Ru(0001), and Rh(111).

The reaction barriers associated with TS(a) and TS(b) in Figure 2 were found to be 0.93 (90 kJ/mol) and 1.02 eV (98 kJ/mol), respectively. These values are very close to reaction barriers determined on Pt(111),[16,19] indicating the similar reactivities of Pd and Pt for CO oxidation, as suggested experimentally.[44] Considering that CO oxidation may take place at the boundries between O_a islands and CO islands, we also studied the reaction in Pd(111)−(4 × 2)−(O_a + CO) unit cells. This unit cell which contains two separate domains, (2 × 1)−CO and (2 × 1)−O_a, allowed us to further test the validity of the p(2 × 2) model. The initial state was found to be the one with O_a on fcc sites and CO also on fcc sites, which is the same as that found in Pd(111)−(2 × 2)−(O_a + CO). The TS structure is also very similar with that identified in Pd(111)−(2 × 2)−(O_a + CO): O_a is near a bridge site and the CO is slightly off the top site. The lowest energy reaction barrier was calculated to be 0.89 eV, which is only slightly lower than that of 0.93 eV obtained in the (2 × 2) unit cell.

3.2. CO Oxidation on Pd(111) at an O Coverage of 1/6 ML. To study what effect surface coverage has on the CO oxidation reaction and to make a comparison with the reaction pathways on Pd(100) described in the next section, we reduced the coverage of the adsorbates and performed DFT calculations in a p(3 × 2) unit cell (both O and CO coverges are 1/6 ML and the 1/6 ML coverage will hereafter be referred to as this system). It is worth stressing that in the p(3 × 2) unit cell the CO and the O_a are well separated in the initial state and the interaction between them is very small. Therefore, the reaction in this unit cell effectively models CO oxidation at very low surface coverages. Again, the most stable initial state in the p(3 × 2) unit cell was first searched. As shown in Figure 3, with the O_a being on the fcc hollow site there are four possible sites for CO adsorption. Other sites with high bonding competition are ruled out because those systems are less stable than that with low or no bonding competition, as shown in previous work.[16,55,61] For example, the fcc hollow site for CO adsorption was not calculated because CO on the fcc site and O_a on another fcc site would share some bonding with the same metal atoms

(61) Bleakley, K.; Hu, P. *J. Am. Chem. Soc.* **1999**, *121*, 7644.

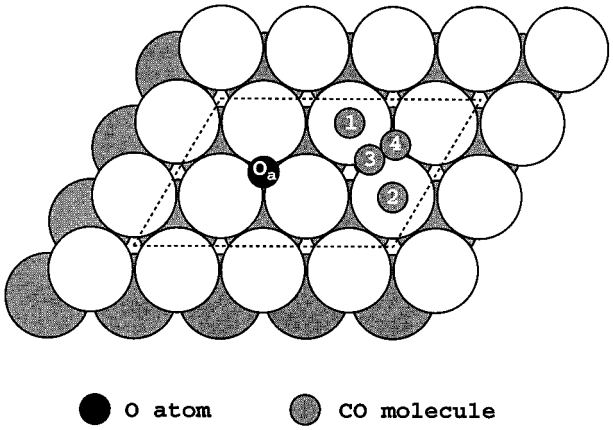

Figure 3. Four possible adsorption sites for CO with O_a being on the fcc hollow site in Pd(111)−p(3 × 2)−(CO + O_a): (1) top site; (2) another top site; (3) bridge site;and (4) hcp hollow site. The large white circles and the large gray circles represent the first and second layer of Pd atoms, respectively. The small gray circle and small dark circle indicate CO and O_a, respectively. The unit cell in the surface plane is indicated with dotted lines.

which increases the energy of the coadsorption system. We have checked the four CO adsorption sites. A summary of chemisorption energies of CO and O_a in these coadsorption systems is shown in Table 1. It can be seen that the most stable structure is when CO locates on the hcp hollow site with the O_a being on the fcc hollow site. This agrees with the experiments[38,39] which find that the hollow site is the preferred site for CO adsorption on Pd(111) at low coverages.

Since TS(a) (Figure 2a) is more stable than TS(b) (Figure 2b) at 1/4 ML coverage, we only carried out a search for the type of TS(a) in the p(3 × 2) unit cell. A very similar TS to TS(a) was identified. The O_a atom was also found to be close to a bridge site with the CO on an off-top site. The distance between C and O_a was 1.80 Å, which is identical with that of TS(a) obtained in the p(2 × 2) unit cell. The angle between O_a−C and C−O is 113.1°, which is similar to that in the p(2 × 2) unit cell (114.4°). The main structural parameters of the TS at 1/6 ML coverage are listed in Table 2. The reaction barrier at this coverage was determined to be 1.49 eV (144 kJ/mol), which is much higher than that obtained at 1/4 ML coverage.

3.3. CO Oxidation on Pd(100) at an O Coverage of 1/4 ML. In addition to the systems investigated on Pd(111), analogous simulations were performed on Pd(100). The most stable initial state of the reaction on Pd(100) within a p(2 × 2) unit cell was first searched. Two structures with low energies have been obtained. One structure has O_a on a hollow site and CO on a bridge site. The other has both O_a and CO on hollow sites (Figure 4). The energy difference between these two structures was found to be very small, as can be seen from the similar chemisorption energies of O_a and CO in each structure listed in Table 3. The relevant data reported in the literature[59,60,62] are also listed in Table 3.

Having determined the most stable initial state, possible TSs were searched. Three distinct TSs were found, which are schematically illustrated in Figure 5. The main structural parameters of these TSs are listed in Table 4. In TS(a) (Figure 5a), the O_a atom is near a bridge site and the CO is near an opposite bridge site. The distance between the O_a and the CO is 2.00 Å. The reaction barrier was determined to be 0.78 eV (75 kJ/mol). In TS(b) (Figure 5b), the O_a atom is also near a bridge site and the CO is close to the nearest bridge site. The

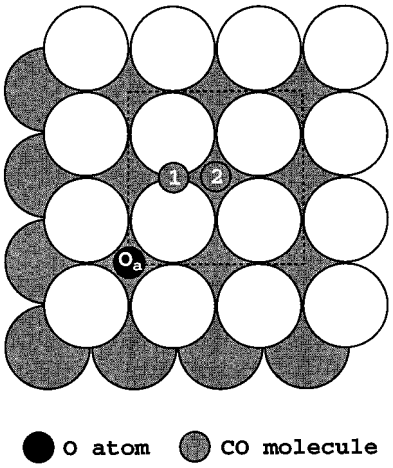

Figure 4. Top view of two initial state structures for CO oxidation in Pd(100)−p(2 × 2)−(CO + O_a): (1) CO is on the bridge site and (2) CO is on the hollow site, with the O_a being on a hollow site. The large white circles and the large gray circles represent the first and second layer of Pd atoms, respectively. The small gray circle and small dark circle indicate CO and O_a, respectively. The unit cell in the surface plane is indicated with dotted lines.

Table 3. Chemisorption Energies of O_a and CO in Pd(100)−p(2 × 2)−(CO + O_a) and Pd(100)−p(3 × 2)−(CO + O_a)[a]

	chemisorption energy (eV)	
	O_a	CO
Pd(100)−p(2 × 2)−(CO + O_a)		
1 CO bridge; O_a hollow	3.97	2.02
2 CO hollow; O_a hollow	4.07	2.12
Pd(100)−p(3 × 2)−(CO + O_a)		
1 CO top; O_a hollow	4.30	1.69
2 CO bridge; O_a hollow	4.23	2.17
3 CO another bridge; O_a hollow	4.37	2.31
Pd(100)−c(2 × 2)−O(hollow)[b]	3.77	
Pd(100)−p(2×2)−O(hollow)[c]	4.14	
Pd(100)−p(2 × 2)−CO(bridge)[c]		1.98
Pd(100)−c(2 × 2)−CO(bridge)[d]		1.92

[a] The chemisorption energies of O_a and CO are defined in a similar way to those described in Table 1. There are two and three possible coadsorption structures with low energies in p(2 × 2) and p(3 × 2) unit cells, respectively, which correspond to the structures shown in Figures 4 and 6, respectively. For comparison, some relevant data from the literature are also listed. [b] Reference 59. [c] Reference 60. [d] Reference 62.

reaction barrier associated with this TS was found to be 1.24 eV (119 kJ/mol), being much higher than that of TS(a). The third TS, TS(c), is shown in Figure 5c. Unlike TS(a) and TS(b) where O_a and CO are near bridge sites, the O_a atom in TS(c) is only slightly away from the initial hollow site along the C−O_a axis and the CO is on an off-top site. Another interesting feature of TS(c) that we will discuss later is the large relaxation of the top metal layer in the surface plane. In this TS, the bond distance between the C and the O_a was found to be 1.82 Å and the reaction barrier associated with it is 1.02 eV (98 kJ/mol). Considering the large relaxation in the top layer of Pd in TS(c), shown in Figure 5c, calculations were also conducted in which both the top and second layers of Pd atoms were allowed to relax. It was found that the TS geometry is very similar with TS(c). For example, the C−O_a distance in the new TS differs only by 0.01 Å from that in TS(c). The reaction barrier was calculated to be 0.96 eV (1.02 eV from TS(c)). These results indicate that the relaxation of the second Pd layer has little effect on the reaction pathway and barrier.

3.4. CO Oxidation of Pd(100) at an O Coverage of 1/6 ML. In the p(2 × 2) unit cell, CO and O_a share some bonding

(62) Eicher, A.; Hafner, J. *Phys. Rev. B* **1998**, *57*, 10110.

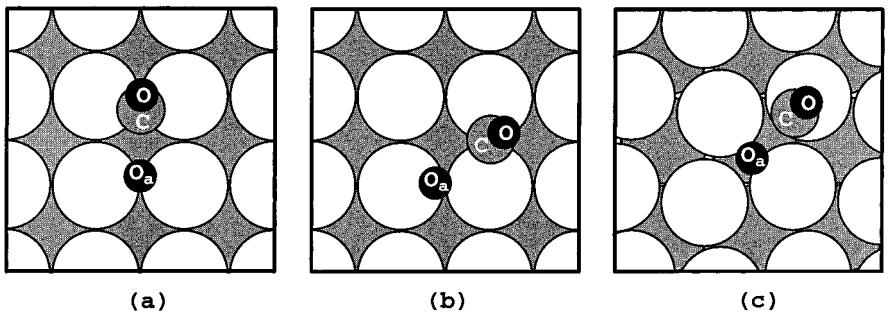

Figure 5. Three distinct transition state geometries for CO oxidation on Pd(100). The main structural parameters are listed in Table 4.

Table 4. The Main Geometrical Parameters of the TSs Identified for CO Oxidation on Pd(100) in p(2 × 2) and p(3 × 2) Unit Cells and the Reaction Barriers Associated with These TSs

	barrier (eV)	C−O_a (Å)	C−Pd (Å)	C−O (Å)	∠O_a−C−O (deg)
TS(a)					
1/4 ML	0.78	2.00	2.03	1.17	106.5
1/6 ML	1.05	1.98	2.05	1.17	107.5
TS(b)					
1/4 ML	1.24	1.90	2.07	1.17	109.9
TS(c)					
1/4 ML	1.02	1.82	1.95	1.17	97.5

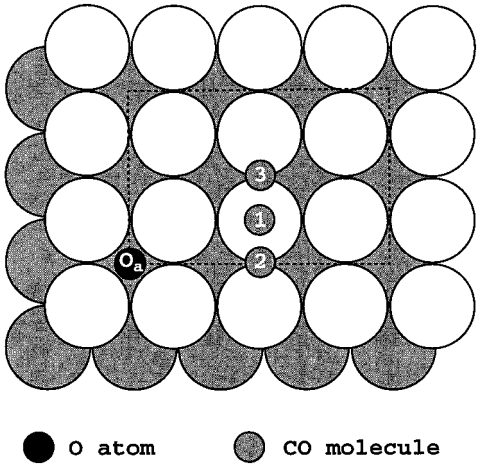

Figure 6. Three possible adsorption sites for CO with O_a being on a hollow site in Pd(100)−p(3 × 2)−(CO + O_a): (1) top site; (2) bridge site; and (3) another bridge site. The large white circles and the large gray circles represent the first and second layer of Pd atoms, respectively. The small gray circle and small dark circle indicate CO and O_a, respectively. The unit cell in the surface plane is indicated with dotted lines.

with the same metal atom in the initial state (Figure 4), which may increase the total energy of the initial state and thus affect the reaction barrier. Therefore, we carried out calculations in a larger unit cell, a p(3 × 2). As shown in Figure 6, there are also several possible initial states with low energies for CO adsorption with O_a being on the hollow site: The CO can be on bridge sites or a top site. We performed structure optimizations for all three coadsorption systems and chemisorption energies of O_a and CO for each system are shown in Table 3. As can be seen, the most stable system is the structure with O_a on the hollow site and CO on a bridge site. The result that the CO chemisorbs preferentially on the bridge site is consistent with the experimental observation.[33−35] As described above, TS(a) (Figure 5a) has the lowest energy among the three identified TSs in the p(2 × 2) unit cell. Therefore, in the p(3 × 2) unit cell we carried out a search for this TS alone. A similar TS, also with the O_a near a bridge site and the CO near an opposite bridge site, has been located. The main structural parameters in this TS are listed in Table 4. The bond distance between C and O_a was calculated to be 1.98 Å, very close to that of TS(a) obtained in the p(2 × 2) unit cell (2.00 Å). The reaction barrier associated with this TS in the p(3 × 2) unit cell was calculated to be 1.05 eV (101 kJ/mol).

4. Discussions

4.1. Surface Structure Effects on Reaction Pathways. As discussed in section 3.1, a crucial event in CO oxidation on close-packed surfaces is the activation of O_a from a 3-fold hollow site toward a bridge site. By a careful examination of the TSs of CO oxidation on Pd(100), shown in Figure 5, a similar feature emerges: The O_a atom must be near a bridge site. This is obviously true in TS(a) and TS(b). TS(c) is an intriguing one. Although in TS(c) the O_a is just slightly off the initial hollow site, it can be approximately considered as a bridge site O_a on a (111)-like surface because of the large deformation of the surface plane of Pd(100): Compared to the initial state, the distance between the two metal atoms along the C−O_a axis in the top layer is elongated by ca. 0.5 Å and the distance of the other two metal atoms perpendicular to the C−O_a axis is shortened by ca. 0.4 Å. The top metal layer, therefore, becomes a (111)-like surface plane (Figure 5c). In fact, TS(c) on Pd(100) is similar to the TSs located on Pd(111).

To obtain further insight into the reaction pathways on Pd(100), we have examined the electronic structures of different states in CO oxidation on Pd(100) at 1/4 ML coverage. We carried out calculations for three structures, O_a in the initial state (O_a/IS), TS(a) (O_a/TS(a)), and TS(c) (O_a/TS(c)), which are exactly the same as the initial state, TS(a) and TS(c) on Pd(100) in the p(2 × 2) unit cell, respectively, except that the CO has been removed. Plots of local density of states (LDOS) projected onto the O_a atom versus energy from these systems are shown in Figure 7. The dotted curves correspond to O_a/IS, and the solid curves in Figure 7a,b correspond to O_a/TS(a) and O_a/TS(c), respectively. These LDOS for O_a/TS(a) and O_a/TS(c) are calculated by cutting a small volume (0.1 Å radius) around a point 0.4 Å away from the O_a atom center, which is the distance between the O_a atom center and the charge density maximum of O_a p orbitals, along the directions as the O_a−CO bond axis in the TSs. Similar calculations are performed for O_a/IS with the center of the volume again centered 0.4 Å away from O_a in the O_a−CO plane (the directions are shown in the insets in Figure 7). By examining the individual quantum states of the systems, we found that the first peak in each system from the left-hand side contains almost exclusively O_a 2s character. The large intensity of the peak indicates a high localization of electrons around the O_a atom. The second peak (∼−5 eV) consists of p(O_a)−d(Pd) bonding states. Figure 7 shows clearly that when O_a is on the initial hollow site (the dotted curves),

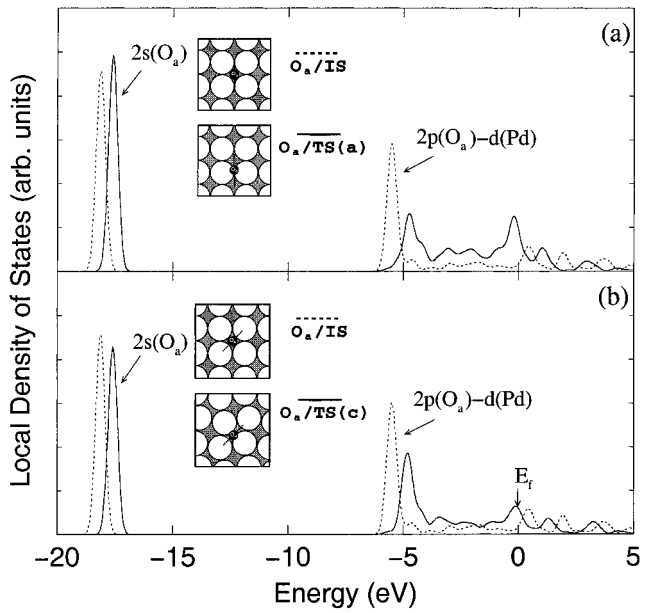

Figure 7. LDOS projected onto the O_a atom in O_a/IS (dotted curves in parts a and b), O_a/TS(a) (solid curve in part a), and O_a/TS(c) (solid curve in part b), where O_a/IS, O_a/TS(a), and O_a/TS(c) are defined in the text. The zero on the energy axis corresponds to the Fermi level. The lines in the insets indicate the projection directions of the LDOS in different systems.

high charge densities are located in the low-energy p orbitals of O_a while the charge densities between −4 eV and the Fermi level are relatively small. This indicates that when O_a is on the hollow site, it bonds strongly with the metal atoms and is reluctant to form new bonds with CO. In the case of the O_a near the bridge site (TS(a)), however, as shown in Figure 7a, the charge densities of the second peak (∼-5.0 eV) are decreased considerably (the solid curve). This indicates that at this site the O_a−Pd bonding is significantly weakened and some new bonding between O_a and CO is then possible. Obviously, O_a activation from the initial hollow site toward a bridge site is a crucial feature for the reaction on Pd(100). Even in the case of O_a/TS(c), although the O_a is just slightly away from the initial hollow site, the deformation of the top metal surface, especially the elongation of the distance between the two metal atoms along the C−O_a axis, results in the O_a being on a bridge-like site. In this case, the O_a−Pd bonding is considerably weakened, as evidenced by the reduced O_a p electron densities at low energies (the solid curve in Figure 7b). These features agree with the analyses performed on close-packed metal surfaces,[23] which also showed the necessity for O_a activation. In addition to O_a activation, the CO movement is also found to be important in the reaction pathway on Pd(100). In both TS(a) and TS(b), the CO has to be near a bridge site. The nearest bridge site (TS(b)), however, is not favored compared to the opposite bridge site (TS(a)). In TS(c), the CO has to be near a top site. Comparing CO oxidation on Pd(100) to that on close-packed transition metal surfaces, therefore, we conclude that the reaction pathways on these surface possess crucial common features.

From Figure 7 it can be seen that the intensity of the second LDOS peak for O_a/TS(a) is smaller than that of O_a/TS(c). This indicates that O_a at TS(a) is more reactive than it is at TS(c), which is consistent with the reaction barriers shown in Table 4 (0.78 and 1.02 eV for TS(a) and TS(c), respectively). It is worth mentioning that the reaction barrier for TS(b) is substantially higher than that for TS(a), although the O_a atom is in a similar position in both TSs. This can be rationalized in terms of bonding competition.[16,55,61] In TS(b), O_a and CO have to share bonding with one metal atom (Figure 5b). This causes a significant bonding competition and thus the energy of the TS is quite high. In TS(a), however, O_a and CO do not have to share bonding with the same metal atom and thus the energy of the TS is relatively low.

Finally, it is interesting to compare the structures of the two lowest energy TSs identified on the (100) and (111) surfaces (TS(a) in Figure 2a and TS(a) in Figure 5a). These TSs are actually very similar in nature: O_a is near a bridge site and CO lies in a plane perpendicular to the Pd−Pd bond of the bridge site; and the O_a−C distance is around 1.80−2.00 Å and the O_a−C−O angle is around 110° in both TSs. Moreover, as discussed above and in previous work,[23] the movement of O_a from the initial hollow site toward a bridge site is found to be a common feature on both the (100) and (111) surfaces. It will be interesting to see how far these TSs' features can be extended to other surfaces. It is possible that TSs with similar structures will be observed on other surfaces, for example, (110) surfaces.

4.2. Surface Structure Effects on Reactivity. Although CO oxidation on Pd(100) and Pd(111) possesses the same crucial features, the reactivities of these two surfaces are not always the same. At 1/4 ML coverage, the barriers on both surfaces are similar (0.93 eV on Pd(111) and 0.78 eV on Pd(100)), whereas at 1/6 ML coverage, there is as much as a 0.44 eV difference between them (1.49 eV on Pd(111) and 1.05 eV on Pd(100)). Therefore, an interesting question arises: Why is the reaction barrier on Pd(111) considerably high compared to that on Pd(100) at lower coverages whereas they are similar at higher coverages?

It has been suggested[16,63,64] that the reaction barrier is related to the O−metal bond strength. For instance, this argument can be used to explain the different reactivities of Pt and Ru for CO oxidation: Because the O−metal bonding on a Ru surface is considerably stronger than that on Pt, the reaction barrier for CO oxidation on Ru is significantly higher than that on Pt.[16,21] However, this argument does not sit comfortably with our results at lower coverages. As shown in Tables 1 and 3, the chemisorption energy of O_a on Pd(100) (4.37 eV, 422 kJ/mol) is similar to that on Pd(111) (4.18 eV, 403 kJ/mol), while the barrier obtained on Pd(100) is much lower than that on Pd(111) at 1/6 ML coverage. Considering the two crucial events in the reaction pathways concluded from our calculations, the O_a activation and the appropriate CO movement, we argue that the reaction barrier is actually related to the energy changes caused by the movements of both species from the initial state to the TS. In other words, the barrier is determined by the actual pathway of the reaction. This argument can be used to explain why the reaction barrier on Pd(111) is considerably high compared to that on Pd(100) at low coverages. For the reaction on Pd(100) at 1/6 ML coverage, initially the O_a is on the hollow site with the CO being on a bridge site. At the TS, the O_a is near a bridge site with the CO being close to another bridge site. Therefore, the reaction barrier would mainly be ascribed by the O_a movement. In the case of Pd(111), the O_a movement is very similar to that of the (100) surface whereas the CO movement is quite different: Initially the CO is on a hollow site and at the TS the CO is close to a top site at 1/6 ML coverage. Therefore, the barrier would be determined by the movements of both the O_a and the CO. In particular, because

(63) Yoshinobu, J.; Kawai, M. *J. Chem. Phys*. **1995**, *103*, 3220.
(64) Bottcher, A.; Niehus, H.; Schwegmann, S.; Over, H.; Ertl, G. *J. Phys. Chem. B* **1997**, *101*, 11185.

the chemisorption energy difference between the hcp and top sites is quite large on Pd(111) (CO chemisorption energy in Table 1: 1.43 eV on the top site and 2.13 eV on a hcp hollow site), CO movement from the hcp hollow site to the off-top site (from the initial state to the TS) costs a significant amount of energy, resulting in a high reaction barrier on Pd(111).

Based on the above analysis, we propose the following equation to estimate the reaction barrier:

$$E_a = E_O + E_{CO} + E_{surf} + E_m$$

where E_a is the reaction barrier, E_O and E_{CO} are the energies required to activate O_a and CO, respectively, from the initial state to the TS, E_{surf} is the energy associated with surface relaxation during the reaction, and E_m is a mixing term that includes the O_a-CO bond formation energy and an energy due to bonding competition.[16,55,61] At medium and high coverages, E_{CO} is small and the contribution from E_O was calculated to be similar on both Pd(111) and Pd(100). E_{surf} was estimated from the energy difference between a clean surface with the TS structure and that with the initial state structure. It was found to be small ($\sim$0.1 eV) from both Pd(100) and Pd(111). E_m is metal dependent and is related to the TS structure. As mentioned in the last section, the TS structures with the lowest reaction barriers on Pd(111) and Pd(100) are very similar. Therefore, E_m is expected to be similar on both surfaces. Consequently, the reaction barriers on both surfaces are similar at medium or high coverages. On the other hand, at low coverages, the major difference in E_a between Pd(111) and Pd(100) lies in the second term, E_{CO}. E_{CO} is small ($\sim$0.1 eV) for Pd(100) but quite large ($\sim$0.7 eV) for Pd(111), resulting in the quite different barriers for these two surfaces.

It is interesting to note that our calculations show that as surface coverage decreases, the change of the reaction barrier on Pd(100) is relatively small (from 0.78 eV at 1/4 ML coverage to 1.05 eV at 1/6 ML coverage), while a quite dramatic change in reaction barrier on Pd(111) can be seen (from 0.93 eV at 1/4 ML coverage to 1.49 eV at 1/6 ML coverage). This result can be rationalized as follows. As shown in Tables 2 and 4, the change of the surface coverages does not have a large impact in the TS structures on both Pd(111) and Pd(100). However, it does affect the initial states. Our calculations show that the initial state on Pd(100) at 1/6 ML is slightly more stable than that at 1/4 ML coverage, as evidenced by only about 0.2 eV difference of CO (or O_a) chemisorption energy between 1/6 and 1/4 ML coverage. Therefore, the reaction barrier increases slightly. On the other hand, the initial state on Pd(111) at 1/6 ML coverage is much more stable than that at 1/4 ML coverage, as evidenced by an ca. 0.5 eV difference of CO (or O_a) chemisorption energy between the two coverages. This leads to a large increase in the reaction barrier.

5. Conclusion

In summary, this study represents one of the first attempts to investigate surface structure effects on both reaction pathways and reactivity. Specifically, a detailed comparison between the reaction mechanisms of CO oxidation on Pd(100) and Pd(111) has been made. It is concluded that the reaction pathways on both surfaces possess common features. Surface coverage affects the reactivity of CO oxidation on Pd(111) considerably while it has little effect on Pd(100). The reaction is found to be structure insensitive at medium or high coverages, while it is structure sensitive at low coverages.

Acknowledgment. We gratefully acknowledge the Supercomputing Center in Ireland for computing time. We also thank the EPSRC for financial support.

JA002432F